DISCRETE AND CONTINUOUS
DYNAMICAL SYSTEMS SERIES B
Volume **13**, Number **2**, March **2010**

doi:10.3934/dcdsb.2010.13.347

pp. **347–373**

INTEGRATORS FOR HIGHLY OSCILLATORY HAMILTONIAN SYSTEMS: AN HOMOGENIZATION APPROACH

Claude Le Bris

Université Paris-Est, CERMICS, Ecole Nationale des Ponts et Chaussées
6 et 8 avenue Blaise Pascal, 77455 Marne-la-Vallée Cedex 2, France, and
INRIA Rocquencourt, MICMAC team-project, 78153 Le Chesnay Cedex, France

Frédéric Legoll

Université Paris-Est, Institut Navier, LAMI, Ecole Nationale des Ponts et Chaussées
6 et 8 avenue Blaise Pascal, 77455 Marne-la-Vallée Cedex 2, France, and
INRIA Rocquencourt, MICMAC team-project, 78153 Le Chesnay Cedex, France

(Communicated by Gregoire Allaire)

Abstract. We introduce a systematic way to build symplectic schemes for the numerical integration of a large class of highly oscillatory Hamiltonian systems. The bottom line of our construction is to consider the Hamilton-Jacobi form of the Newton equations of motion, and to perform a two-scale expansion of the solution, for small times and high frequencies. The approximation obtained for the solution is then used as a generating function, from which the numerical scheme is derived. Several options for the derivation are presented. The various integrators obtained are tested and compared to several existing algorithms. The numerical results demonstrate their efficiency.

1. **Introduction.** This article presents a possible systematic methodology to design symplectic algorithms for a large class of highly oscillatory Hamiltonian dynamics. In short, our methodology consists in considering the Hamilton-Jacobi form of the Newton equations of motion, and performing a two-scale expansion of the solution, for small times and high frequencies.

The specific form of Hamiltonian systems we consider in this work reads

$$H_\varepsilon(q_1,q_2,p_1,p_2) = \frac{p_1^T p_1}{2} + \frac{p_2^T p_2}{2} + V_0(q_1,q_2) + (\Omega(q_1))^2\ \frac{q_2^T q_2}{2\varepsilon^2}, \tag{1}$$

where ε is a small parameter ($\varepsilon \ll 1$), where $q = (q_1, q_2) \in \mathbb{R}^s \times \mathbb{R}^f$ and $p = (p_1, p_2) \in \mathbb{R}^s \times \mathbb{R}^f$ (the superscripts s and f respectively stand for the slow and the fast variables), and where V_0 is a potential energy that does not depend on ε, and is bounded from below. The important assumption in (1), which limits the applicability of our work, lies in the specific form of the Hamiltonian (1) regarding the fast degrees of freedom. It is assumed to be a *harmonic* oscillator,

$$\frac{p_2^T p_2}{2} + (\Omega(q_1))^2\ \frac{q_2^T q_2}{2\varepsilon^2}, \qquad \text{in those fast degrees of freedom.}$$

2000 *Mathematics Subject Classification.* Primary: 70K70, 37M15, 70H20, 65P10.
Key words and phrases. Numerical schemes, highly oscillatory Hamiltonian systems, generating function, two-scale expansion, symplectic algorithms.

In addition, but this time this is not such a strong, structural assumption, we assume throughout this article that the fast frequency $\Omega(q_1)$ is a scalar quantity, and that there exists $c > 0$ such that $\Omega(q_1) \geq c > 0$ for all q_1. The case where $(\Omega(q_1))^2 \, \frac{q_2^T q_2}{2\varepsilon^2}$ is replaced by $\frac{q_2^T \Omega^2(q_1) q_2}{2\varepsilon^2}$, where $\Omega(q_1)$ is a symmetric $f \times f$ matrix, is, in principle, tractable with our approach, but leads to several difficulties that we have not been able to satisfactorily solve yet.

Our last assumption is that, for consistency, the initial conditions of the Hamiltonian dynamics derived from (1) are assumed to depend on ε in such a way that the system energy is bounded with respect to ε. In particular, this implies that q_2 is of order ε at initial time, a property that is propagated forward in time. We shall comment upon the above three assumptions below.

As is well-known, the numerical integration of the Newton equations derived from (1), namely

$$\frac{dq}{dt} = \frac{\partial H_\varepsilon}{\partial p}(q,p), \quad \frac{dp}{dt} = -\frac{\partial H_\varepsilon}{\partial q}(q,p), \tag{2}$$

using a standard symplectic scheme (such as velocity Verlet) is expensive. This originates from the smallness of ε, which dramatically reduces the size of admissible time steps.

Our purpose is thus to design numerical integrators that are much more efficient. There already exist many works in this direction. Indeed, Hamiltonian systems of the type (1) have already been studied in the literature, see for instance [2, 3, 21]. In [21, Chap. XIII and XIV], E. Hairer, Ch. Lubich and G. Wanner present in a unified way and analyze several algorithms designed for the integration of (2). Another algorithm, which also belongs to the class that is analyzed in [21], has been proposed in [14]. The Hamiltonian (1) has also been considered in [4], where an averaging technique is used to build a different algorithm. We also mention the studies [9, 33], based on the Heterogeneous Multiscale Method paradigm, the Equilibrium method [22], and the methods proposed in [26, 30]. In contrast to the above works, and as announced above, our idea, in order to derive efficient algorithms for Hamiltonian systems which are symplectic *by construction*, is to work on the Hamilton-Jacobi form of the equations of motion. Otherwise stated, we adapt to the case of highly oscillatory systems the idea originally used by Feng in [10] to build symplectic integrators. In fact, we will superimpose to the latter the idea of two-scale expansion, natural in such a multiscale context.

Some important comments are already in order, both on our purpose and on the assumptions we make.

First, let us discuss in its own the purpose of constructing symplectic integrators for such multiscale Hamiltonian systems.

Certainly, symplectic schemes are natural for the integration of Hamiltonian systems since they reproduce at the discrete level an important geometric property of the exact flow. More than natural, symplectic schemes are also proved to be efficient as regards the conservation of the energy and of the possible invariants of the system over extremely long times (see [21, Chap. IX and X] and [1, 17, 31]; see also [16] where, on a numerical example, symplectic methods are shown to be superior to some non-symplectic methods that exactly preserve the energy). The proof of this property, as is well-known, relies on backward error analysis (along with some elements of KAM theory, for the conservation of the invariants). In any case, the properties of conservation are obtained in the limit of small time steps. This is

where our context of highly oscillatory equations somehow collides with the above line of thought. For backward error analysis to hold true, the time step has to be small compared to ε (the shortest period present in the system), but, for efficiency, the time step used in practice needs to be much larger than ε. So, we will not be able to refer to backward error analysis to justify the long time conservation properties of the scheme. The notion of symplecticity in its own may even be considered of poor interest in this particular context (see the introduction of Chapter XIII of [21]). Ideally, what we would need is a notion of *partial symplecticity* with respect to the slow degrees of freedom in the system. In the absence of such a notion, and of the corresponding construction, the best we can do is build a "globally" symplectic scheme, and *observe* its actual conservation properties.

Another property that could be of interest, alternatively to symplecticity, is *symmetry*. In the case of a constant fast frequency, we build a non-symmetric scheme (see Algorithm 2.1 below), and also consider its symmetrized version (see Algorithm 2.2). In the general case of a non constant fast frequency, the scheme we propose, namely Algorithm 3.1, is not symmetric. At present time, it is not clear, to us at least, how symmetry is related to long time conservation properties. The literature does not seem to provide a definite understanding of this issue: examples [18] and counterexamples [11] exist, showing the complexity of the situation. Despite such a growing literature, the understanding of symmetric methods is not at the level of that of symplectic methods. In addition, symmetric schemes are often implicit.

A last general point we would like to emphasize, before getting to some other types of comments, is that we are after the computations of *trajectories*. Our purpose here is *not* to build a reduced system, involving only the slow degrees of freedom in the presence of some effective potential created by the (eliminated) fast degrees of freedom. We do not want either to directly compute averages based on the trajectories. For both above issues, there are a lot of relevant, excellent, studies and approaches in the literature. The only question we address here is: are we able, while keeping all the degrees of freedom explicit, to approximate as accurately as possible the trajectories over long times?

Second, let us briefly comment upon our assumptions. There are three of them: the form of the Hamiltonian, the form of the fast frequency $\Omega(q_1)$, the size of the initial conditions.

Our approach applies to Hamiltonians that are *harmonic in the fast variables*. Although this specific form is quite general, and already used in the literature (see e.g. [4, 14]), we conceed that this is a strict, structural, limitation of our work. This is related to our technique of derivation. The harmonicity of the Hamiltonian with respect to the fast degrees of freedom translates into the (partial) periodicity of the generating function S_ε, a property that is subsequently used to close the hierarchy of equations produced by the two-scale expansion (see Section 2.1). Somehow, this harmonicity hypothesis *assumes* that some preliminary work has been performed on the original Hamiltonian in order to approximate its fast degrees of freedom. It is not *a priori* impossible that some analogous derivation could be performed for slightly more general Hamiltonians. In homogenization theory, it is indeed well-known that periodicity is an assumption that may be relaxed in various directions (think of *stochastic* homogenization, ...). However, it is unlikely that *all* Hamiltonians will be tractable with such an approach. This has the following consequence: in order to compare the integrators we derive with other, more generic integrators (such as

the Impulse method [15, 34] or the Mollify method [12, 32]) in a fair manner, we will bear in mind the specificity of our setting.

Our second assumption concerns the fast frequency $\Omega(q_1)$. The expression (1) shows a *scalar* frequency $\Omega(q_1)$. This is the only case we shall consider in this article. In other words, this corresponds to a spherical matrix of frequencies, and to fixed eigenmodes that all share the same eigenvalue. There are several extensions of this simple case (see [21, Chap. XVI], [24, 25, 29], and [23] for the case of a non constant fast frequency, and [21, p 535] for an illustrative and simple example on which eigenvalues of the frequency matrix cross, which induces additional difficulties). The interested reader will find a short review on these different cases in [7]. Clearly, the scalar case that we consider here is rather simple. However, it is rich enough to allow for several interesting variants of our construction.

Regarding initial conditions, we have chosen to work with initial conditions whose energy is bounded, uniformly in ε. As already mentioned, this implies that the position q_2 of the fast variable is also bounded from above by ε. Therefore, the nonlinear feedback it might have on the slow degrees of freedom, *via* the potential $V_0(q_1, q_2)$, is all the smaller. We will thus take care of testing the integrators over an extremely long time frame, so as to let the possible instabilities develop, if they have to.

Finally, and in addition to this list of comments, let us emphasize one, extremely important mathematical point, not to say weakness, in our derivation. We are unable to perform any numerical analysis of our algorithms. This would clearly provide a rigourous understanding. We are only in position to test the integrators numerically, and observe their remarkable efficiency. Actually, to the best of our knowledge, it seems that the only numerical analysis tool that is available in the context of highly oscillatory Hamiltonian systems is the Modulated Fourier Expansion (MFE) (see [21, Sec. XIII.5], [5, 6, 20]), which currently works well to analyze certain symmetric schemes. So, although symmetric schemes are often implicit (such as Algorithm 2.2 that we propose in Section 2.1, which is symplectic, symmetric and implicit), they are interesting because they *may* allow for a numerical analysis.

The plan of our work is as follows. First, in Section 2, we consider the case when the fast frequency is constant. Section 2.1 describes the derivation of two algorithms and Section 2.2 shows the numerical results on some commonly used test case. Next, in Section 3, we address the case when the fast frequency actually depends on the slow position q_1. We hope to be able to return in future publications to other, more complicated, cases of fast frequencies. Note that the methodology described here in details has been introduced in [27]. We also outlined there the derivation of *some* (but not all) algorithms presented below. Even in the present *extended and updated* version, it is not possible to give all the details of the calculations, which might be rather tedious, although not difficult. They can be read in [28].

We conclude this introduction by some preliminary calculations, which will make the above strategy somewhat more precise.

Let $\overline{S}_\varepsilon(t, q, P)$ be the solution of

$$\partial_t \overline{S}_\varepsilon = H_\varepsilon \left(q + \partial_P \overline{S}_\varepsilon, P \right), \quad \overline{S}_\varepsilon(0, q, P) = 0. \tag{3}$$

For all (q, p, t), we know that $(Q(t), P(t))$, implicitly defined by

$$p = P(t) + \frac{\partial \overline{S}_\varepsilon}{\partial q}(t, q, P(t)), \quad Q(t) = q + \frac{\partial \overline{S}_\varepsilon}{\partial P}(t, q, P(t)), \tag{4}$$

solve (2) with the initial conditions (q,p). At this stage, we are in position to more explicitly describe our approach. Using a two-scale type Ansatz, we derive an approximation $\widetilde{S_\varepsilon}(h,q,P)$ of the solution $\overline{S}_\varepsilon(h,q,P)$ of (3) at time $t=h$, for a small parameter ε and for a time step h which is small yet much larger than ε (hence the computational efficiency). Once obtained, this approximation is inserted in the change of variables (4) and a symplectic integrator for (1)-(2) follows. More precisely, in view of (4), we consider the equations

$$p = P_h + \frac{\partial \widetilde{S_\varepsilon}}{\partial q}(h,q,P_h), \quad Q_h = q + \frac{\partial \widetilde{S_\varepsilon}}{\partial P}(h,q,P_h) \tag{5}$$

that define a symplectic map $\widetilde{\Psi}_h : (q,p) \mapsto (Q_h,P_h)$. The corresponding scheme reads $(q_{n+1},p_{n+1}) = \widetilde{\Psi}_h(q_n,p_n)$.

Before we proceed, we need to make a slight preparation. As we have already noticed, the variable q_2 is of order ε, because the energy is bounded. It is thus appropriate to proceed with a change of variable and of unknown function in (3). We set

$$r_2 = \frac{\Omega(q_1)}{\varepsilon} q_2 \quad \text{and} \quad S_\varepsilon(t,q_1,r_2,P_1,P_2) = \overline{S}_\varepsilon\left(t,q_1,\frac{\varepsilon r_2}{\Omega(q_1)},P_1,P_2\right).$$

It follows that, in this new set of variables, S_ε satisfies

$$\begin{aligned} \partial_t S_\varepsilon = \quad & \frac{P_1^T P_1}{2} + \frac{P_2^T P_2}{2} + V_0\left(q_1 + \partial_{P_1} S_\varepsilon, \frac{\varepsilon r_2}{\Omega(q_1)} + \partial_{P_2} S_\varepsilon\right) \\ & + \frac{1}{2}\left(\frac{\Omega(q_1+\partial_{P_1}S_\varepsilon)}{\varepsilon}\right)^2 \left(\frac{\varepsilon r_2}{\Omega(q_1)} + \partial_{P_2} S_\varepsilon\right)^T \left(\frac{\varepsilon r_2}{\Omega(q_1)} + \partial_{P_2} S_\varepsilon\right) \end{aligned} \tag{6}$$

with the initial condition

$$\forall q_1,\ \forall r_2,\ \forall P_1,\ \forall P_2, \quad S_\varepsilon(0,q_1,r_2,P_1,P_2) = 0. \tag{7}$$

This is the form we will use in the sequel.

2. **The case of a constant fast frequency.** In this section, we consider the case when $\Omega(q_1) \equiv \Omega$ does not depend on q_1. A natural idea consists in applying our approach directly on Eq. (6), that is in the original coordinates (q_1,q_2,p_1,p_2). It consists in making the Ansatz

$$\begin{aligned} S_\varepsilon(t,q_1,r_2,P_1,P_2) &= S_0\left(t,\tau,q_1,r_2,P_1,P_2\right) + \varepsilon S_1\left(t,\tau,q_1,r_2,P_1,P_2\right) \\ &+ \text{higher order terms in } \varepsilon^k,\ k \geq 2, \end{aligned}$$

where the fast time τ is

$$\tau = \frac{t\Omega}{\varepsilon}, \tag{8}$$

and where the functions $(S_k)_{k\geq 0}$ are supposed to be 2π periodic in τ. Note that, in the case when V_0 does not depend on q_2, the exact solution to (6)-(7) is consistent with this Ansatz. Indeed, fast and slow variables are then decoupled and the solution to (6)-(7) reads

$$S_\varepsilon = S_{\text{slow}}(t,q_1,P_1) + \varepsilon S_{\text{fast}}(\tau,r_2,P_2),$$

where τ is defined by (8), $S_{\text{slow}}(t,q_1,P_1)$ solves the Hamilton-Jacobi equation

$$\partial_t S_{\text{slow}} = H_1(q_1 + \partial_{P_1} S_{\text{slow}}, P_1), \quad S_{\text{slow}}(0,q_1,P_1) = 0$$

associated to the Hamiltonian $H_1(q_1,p_1) = \dfrac{p_1^T p_1}{2} + V_0(q_1)$, and

$$S_{\rm fast}(\tau, r_2, P_2) = \frac{1}{\Omega}\left[\left(\frac{P_2^T P_2 + r_2^T r_2}{2}\right)\tan\tau + P_2^T r_2\left(\frac{1}{\cos\tau} - 1\right)\right]$$

is indeed 2π periodic in τ and solves the Hamilton-Jacobi equation associated to $H_2(r_2,p_2) = \dfrac{p_2^T p_2}{2} + \Omega^2\,\dfrac{r_2^T r_2}{2}$.

We have followed this idea in [27] (see also [28] for more details). In this article, we follow a different variant of the approach, which actually leads to the most efficient schemes. The idea is to first perform a change of variables, so as to analytically integrate the fast motion, and to only apply our approach in a second stage. Section 2.1 is dedicated to the design of the algorithms. We report on the obtained numerical results in Section 2.2.

2.1. **Derivation of symplectic schemes.** Our approach is suggested by the consideration of the uncoupled case. Indeed, assume momentarily that V_0 does not depend on q_2. Then the fast and the slow variables are decoupled, and we can analytically integrate the fast motion. Such an observation is also used in the exponential integrators analyzed in [21, Chap. XIII], in the integrator described in [14], and in the adiabatic integrators [24, 25] addressing the case of a frequency matrix that varies with q_1. The first step of these algorithms is indeed a change of variables, so that the new variables are solutions of an ODE simpler than the original one.

Consider the time-dependent change of variables $(q_2,p_2) \mapsto (x_2,y_2) = \chi(t,q_2,p_2)$ defined by

$$\begin{aligned} q_2 &= \cos\left(\frac{\Omega t}{\varepsilon}\right) x_2 + \frac{\varepsilon}{\Omega}\sin\left(\frac{\Omega t}{\varepsilon}\right) y_2, \\ p_2 &= -\frac{\Omega}{\varepsilon}\sin\left(\frac{\Omega t}{\varepsilon}\right) x_2 + \cos\left(\frac{\Omega t}{\varepsilon}\right) y_2. \end{aligned}$$

The dynamics on (x_2,y_2) reads

$$\begin{aligned} \dot{x}_2 &= \frac{\varepsilon}{\Omega}\sin\left(\frac{\Omega t}{\varepsilon}\right)\partial_2 V_0\left[q_1(t), \cos\left(\frac{\Omega t}{\varepsilon}\right)x_2(t) + \frac{\varepsilon}{\Omega}\sin\left(\frac{\Omega t}{\varepsilon}\right)y_2(t)\right], \\ \dot{y}_2 &= -\cos\left(\frac{\Omega t}{\varepsilon}\right)\partial_2 V_0\left[q_1(t), \cos\left(\frac{\Omega t}{\varepsilon}\right)x_2(t) + \frac{\varepsilon}{\Omega}\sin\left(\frac{\Omega t}{\varepsilon}\right)y_2(t)\right], \end{aligned}$$

and the dynamics on (q_1,x_2,p_1,y_2) is a Hamiltonian dynamics with the time-dependent Hamiltonian

$$H_\varepsilon^{\rm pre}(t,q_1,x_2,p_1,y_2) = \frac{p_1^T p_1}{2} + W_\varepsilon\left(\frac{\Omega t}{\varepsilon}, q_1, x_2, y_2\right),$$

where

$$W_\varepsilon(\tau,q_1,x_2,y_2) = V_0\left[q_1, (\cos\tau)x_2 + \frac{\varepsilon}{\Omega}(\sin\tau)y_2\right].$$

Let us now take this Hamiltonian, as a function of (q_1,x_2,p_1,y_2), as a starting point for our manipulations. Let $\overline{S}_\varepsilon(t,q_1,x_2,P_1,Y_2)$ solve

$$\partial_t\overline{S}_\varepsilon = \frac{P_1^T P_1}{2} + W_\varepsilon\left(\frac{\Omega t}{\varepsilon}, q_1 + \partial_{P_1}\overline{S}_\varepsilon, x_2 + \partial_{Y_2}\overline{S}_\varepsilon, Y_2\right), \quad \overline{S}_\varepsilon(0,q_1,x_2,P_1,Y_2) = 0.$$

The variable x_2 is of order ε, so we again change of variables and of unknown function:

$$r_2 = \frac{\Omega}{\varepsilon} x_2 \quad \text{and} \quad S_\varepsilon(t, q_1, r_2, P_1, Y_2) = \overline{S}_\varepsilon \left(t, q_1, \frac{\varepsilon r_2}{\Omega}, P_1, Y_2 \right),$$

so that S_ε satisfies

$$\partial_t S_\varepsilon = \frac{P_1^T P_1}{2} + W_\varepsilon \left(\frac{\Omega t}{\varepsilon}, q_1 + \partial_{P_1} S_\varepsilon, \frac{\varepsilon r_2}{\Omega} + \partial_{Y_2} S_\varepsilon, Y_2 \right), \tag{9}$$

with the initial condition $S_\varepsilon(0, q_1, r_2, P_1, Y_2) = 0$. We make the Ansatz

$$\begin{aligned} S_\varepsilon(t, q_1, r_2, P_1, Y_2) = \quad & S_0(t, \tau, q_1, r_2, P_1, Y_2) + \varepsilon S_1(t, \tau, q_1, r_2, P_1, Y_2) \\ & + \text{higher order terms in } \varepsilon^k,\ k \geq 2, \end{aligned} \tag{10}$$

where the fast time τ is again $\tau = \dfrac{t\Omega}{\varepsilon}$, and where the functions $(S_k)_{k\geq 0}$ are supposed to be 2π periodic in τ. We now insert (10) in (9), identify the first variable of W_ε with the fast time τ, and expand in powers of ε.

The fast position is of order ε, so S_0 does not depend on Y_2. From the equation of order ε^{-1}, we infer that S_0 does not depend on τ. The equation of order ε^0 reads

$$\partial_t S_0 + \Omega \partial_\tau S_1 = \frac{P_1^T P_1}{2} + V_0(q_1 + \partial_{P_1} S_0, 0). \tag{11}$$

Since S_0 does not depend on τ and S_1 is 2π periodic in τ, we infer from (11) that

$$\partial_t S_0 = \frac{P_1^T P_1}{2} + V_0(q_1 + \partial_{P_1} S_0, 0) \tag{12}$$

and

$$\partial_\tau S_1 = 0.$$

Equation (12) is supplied with the initial condition $S_0(t = 0, q_1, r_2, P_1) = 0$. For each r_2, we thus recognize the Hamilton-Jacobi equation for the Hamiltonian function

$$H_1(q_1, p_1) = \frac{p_1^T p_1}{2} + V_0(q_1, 0). \tag{13}$$

So S_0 does not depend on r_2. In the sequel, we will approximate $S_0(t, q_1, P_1)$ by

$$S_0(t, q_1, P_1) \approx S_0^{\mathrm{SE}}(t, q_1, P_1),$$

with

$$\begin{aligned} S_0^{\mathrm{SE}}(t, q_1, P_1) &= S_0(0, q_1, P_1) + t \partial_t S_0(0, q_1, P_1) \\ &= t \left(\frac{P_1^T P_1}{2} + V_0(q_1, 0) \right), \end{aligned} \tag{14}$$

which amounts to integrating the Hamiltonian dynamics generated by (13) with the symplectic Euler algorithm. We have $S_0(t) = S_0^{\mathrm{SE}}(t) + O(t^2)$.

The sequel of the identification is rather tedious but not difficult (see [28] for details). We find that

$$S_1 \equiv 0 \tag{15}$$

and that $S_2(t) = S_2^{\rm SE}(t) + O(t^2)$, with

$$\begin{aligned} S_2^{\rm SE}(t,\tau,q_1,r_2,P_1,Y_2) = \quad & \frac{1}{\Omega^2}(\nabla_2 V_0)^T Y_2 - \frac{t}{2\Omega^2}(\nabla_2 V_0)^T \nabla_2 V_0 \\ & + \frac{t}{4\Omega^2}\left(r_2^T \nabla_{22} V_0 r_2 + Y_2^T \nabla_{22} V_0 Y_2\right) \\ & + \frac{1}{\Omega^2}(\nabla_2 V_0(q_1 + tP_1, 0))^T \left((\sin\tau) r_2 - (\cos\tau) Y_2\right), \end{aligned} \tag{16}$$

where the derivatives of V_0 are evaluated at $(q_1, 0)$ unless otherwise mentioned.

Consider now the approximation

$$S_\varepsilon(h) = S_0(h) + \varepsilon S_1(h) + \varepsilon^2 S_2(h) + \ldots \approx S_\varepsilon^{\rm pre1}(h)$$

with

$$\boxed{S_\varepsilon^{\rm pre1}(h) := S_0^{\rm SE}(h) + \varepsilon S_1(h) + \varepsilon^2 S_2^{\rm SE}(h),} \tag{17}$$

where $S_0^{\rm SE}$, S_1 and $S_2^{\rm SE}$ are respectively defined by (14), (15) and (16) (we discuss this choice, and the truncations it implies, in Remark 2 below). We insert this approximation in (5) and obtain the following equations for (P_1, Y_2):

$$\begin{aligned} y_2 = \quad & Y_2 + \frac{h\varepsilon}{2\Omega}\nabla_{22} V_0(q_1,0) r_2 + \frac{\varepsilon}{\Omega}\sin\tau \nabla_2 V_0(q_1 + hP_1, 0), \\ p_1 = \quad & P_1 + h\nabla_1 V_0(q_1,0) + \frac{\varepsilon^2}{\Omega^2}\nabla_{12} V_0(q_1,0) Y_2 - \frac{h\varepsilon^2}{\Omega^2}\nabla_{12} V_0(q_1,0)\nabla_2 V_0(q_1,0) \\ & + \frac{h\varepsilon^2}{4\Omega^2}(r_2^T \nabla_{122} V_0(q_1,0) r_2 + Y_2^T \nabla_{122} V_0(q_1,0) Y_2) \\ & + \frac{\varepsilon^2}{\Omega^2}\nabla_{12} V_0(q_1 + hP_1, 0)\left((\sin\tau) r_2 - (\cos\tau) Y_2\right). \end{aligned}$$

This implicit system reads $z = Z + hf(Z) + \varepsilon g(Z)$ with $z = (p_1, y_2)$, and thus a fixed point method works well to compute $Z = (P_1, Y_2)$. Next, we compute (Q_1, X_2) by explicit formulae. Returning to the original variables (q_1, q_2, p_1, p_2), we write the obtained symplectic scheme as $(Q_1, Q_2, P_1, P_2) = \Psi_h^{\rm pre1}(q_1, q_2, p_1, p_2)$ (see Algorithm 2.1).

Remark 1. High-order derivatives of V_0 appear in Algorithm 2.1. This originates from the strategy of approximating the generating function in order to derive a numerical scheme. This was already observed by Feng [10] for nonstiff Hamiltonian functions of the form $\frac{p^T p}{2} + V(q)$. Replacing such high-order derivatives by their finite difference approximation is a possible option, which however breaks the symplecticity of the scheme if it is done on the scheme itself. Another option is to make this finite difference approximation directly in the generating function, and from there follow (5) to derive a symplectic scheme. We will not pursue in this direction in the present work.

Algorithm 2.1 (Preconditioned Symplectic Scheme $\Psi_h^{\mathrm{pre1}}(q_1,q_2,p_1,p_2)$)**.** Set $(q_1,q_2,p_1,p_2)=(q_1^n,q_2^n,p_1^n,p_2^n)$, $\tau=\Omega h/\varepsilon$ and perform the following steps:

1. Change of variables: set $\quad x_2=q_2, \quad y_2=p_2, \quad r_2=\Omega x_2/\varepsilon$.
2. Solve for (P_1,Y_2) the equations

$$\left\{\begin{array}{ll} y_2= & Y_2+\dfrac{h\varepsilon}{2\Omega}\nabla_{22}V_0(q_1,0)r_2+\dfrac{\varepsilon}{\Omega}\sin\tau\nabla_2V_0(q_1+hP_1,0),\\ p_1= & P_1+h\nabla_1V_0(q_1,0)+\dfrac{\varepsilon^2}{\Omega^2}\nabla_{12}V_0(q_1,0)Y_2\\ & -\dfrac{h\varepsilon^2}{\Omega^2}\nabla_{12}V_0(q_1,0)\nabla_2V_0(q_1,0)\\ & +\dfrac{h\varepsilon^2}{4\Omega^2}(r_2^T\nabla_{122}V_0(q_1,0)r_2+Y_2^T\nabla_{122}V_0(q_1,0)Y_2)\\ & +\dfrac{\varepsilon^2}{\Omega^2}\nabla_{12}V_0(q_1+hP_1,0)\left((\sin\tau)r_2-(\cos\tau)Y_2\right). \end{array}\right.$$

3. Set $Q_1=q_1+hP_1+\dfrac{h\varepsilon^2}{\Omega^2}\nabla_{12}V_0(q_1+hP_1,0)\left((\sin\tau)r_2-(\cos\tau)Y_2\right)$.
4. Set

$$\begin{aligned} X_2 \;=\;& x_2+\frac{\varepsilon^2}{\Omega^2}\nabla_2V_0(q_1,0)+\frac{h\varepsilon^2}{2\Omega^2}\nabla_{22}V_0(q_1,0)Y_2\\ & -\frac{\varepsilon^2}{\Omega^2}\cos\tau\nabla_2V_0(q_1+hP_1,0). \end{aligned}$$

5. Return to the original variables:

$$\left\{\begin{array}{lll} Q_2 & = & (\cos\tau)X_2+\dfrac{\varepsilon}{\Omega}(\sin\tau)Y_2,\\ P_2 & = & -\dfrac{\Omega}{\varepsilon}(\sin\tau)X_2+(\cos\tau)Y_2. \end{array}\right.$$

Set $\left(q_1^{n+1},q_2^{n+1},p_1^{n+1},p_2^{n+1}\right)=(Q_1,Q_2,P_1,P_2)$.

Remark 2. Let us motivate the truncations that we made in the series in powers of ε and h. Since $S_1\equiv 0$, the Ansatz (10) reads

$$S_\varepsilon(h,q_1,r_2,P_1,Y_2)=S_0(h,q_1,P_1)+\varepsilon^2S_2(h,q_1,r_2,P_1,Y_2)+\varepsilon^3e_3(\varepsilon,h,q_1,r_2,P_1,Y_2)$$

with $S_0(h,q_1,P_1)=S_0^{\mathrm{SE}}(h,q_1,P_1)+h^2e_0(h,q_1,P_1)$ and

$$S_2(h,q_1,r_2,P_1,Y_2)=S_2^{\mathrm{SE}}(h,q_1,r_2,P_1,Y_2)+h^2e_2(h,q_1,r_2,P_1,Y_2).$$

Hence, $S_\varepsilon(h)=S_\varepsilon^{\mathrm{pre1}}(h)+E^\varepsilon(h,q_1,r_2,P_1,Y_2)$ with

$$E^\varepsilon(h)=h^2e_0(h)+\varepsilon^2h^2e_2(h)+\varepsilon^3e_3(\varepsilon,h).$$

In view of (5), we have

$$X_2-x_2=\frac{\partial S_\varepsilon(h)}{\partial Y_2}=\frac{\partial S_\varepsilon^{\mathrm{pre1}}(h)}{\partial Y_2}+\frac{\partial E^\varepsilon(h)}{\partial Y_2}.$$

We see that $\partial_{Y_2}S_\varepsilon^{\mathrm{pre1}}(h)$ is a sum of two quantities of respective order ε^2 and ε^2h, whereas $\partial_{Y_2}E^\varepsilon(h)$ is a sum of two quantities of respective order ε^2h^2 and ε^3. Hence $\partial_{Y_2}E^\varepsilon(h)$ is negligible compared to $\partial_{Y_2}S_\varepsilon^{\mathrm{pre1}}(h)$. The same holds true for the equation that defines Y_2. For the slow position, we have

$$Q_1=q_1+\frac{\partial S_\varepsilon^{\mathrm{pre1}}(h)}{\partial P_1}+\frac{\partial E^\varepsilon(h)}{\partial P_1}.$$

The quantity $\partial_{P_1} E^\varepsilon(h)$ includes a term of order h^2, which is not negligible compared to the term of order ε^2 which appears in $\partial_{P_1} S_\varepsilon^{\rm pre1}(h)$. However, since we keep all the terms that come from $S_\varepsilon^{\rm pre1}(h)$ for the fast variables, we also need to keep all of them for the slow variables, in order for the scheme to be symplectic.

Neglecting all terms of order ε^3, the scheme $\Psi_h^{\rm pre1}(q_1,q_2,p_1,p_2)$ is of order 1 in h. A simple, well-known, manner to get a scheme of higher order is to consider the symmetric form

$$(Q_1,Q_2,P_1,P_2) = \Psi_h^{\rm pre2}(q_1,q_2,p_1,p_2) = \left(\Psi_{h/2}^{\rm pre1}\right)^* \ \Psi_{h/2}^{\rm pre1}(q_1,q_2,p_1,p_2).$$

This scheme is symplectic and symmetric and, neglecting all terms of order ε^3, it is of order 2 in h (see Algorithm 2.2). Note that, if V_0 does not depend on q_2, then the slow and the fast variables are decoupled, and we recover the velocity Verlet algorithm in the slow variables and the exact flow in the fast variables.

Algorithm 2.2 (Preconditioned Symplectic Scheme $\Psi_h^{\rm pre2}(q_1,q_2,p_1,p_2)$)**.** Set $(q_1,q_2,p_1,p_2) = (q_1^n,q_2^n,p_1^n,p_2^n)$ and perform the following steps:

1. Set $(\overline{Q}_1,\overline{Q}_2,\overline{P}_1,\overline{P}_2) = \Psi_{h/2}^{\rm pre1}(q_1,q_2,p_1,p_2)$.
2. Set $(Q_1,Q_2,P_1,P_2) = \left(\Psi_{h/2}^{\rm pre1}\right)^* (\overline{Q}_1,\overline{Q}_2,\overline{P}_1,\overline{P}_2)$.

Set $\left(q_1^{n+1},q_2^{n+1},p_1^{n+1},p_2^{n+1}\right) = (Q_1,Q_2,P_1,P_2)$.

Let us conclude this section by the following remark. It is standard to show [2, 3] that the dynamics on the slow variables obtained in the limit $\varepsilon \to 0$ is a dynamics of Hamiltonian $H_1(q_1,p_1) = \dfrac{p_1^T p_1}{2} + V_0(q_1,0)$. We observe that, in the limit $\varepsilon \to 0$, Algorithm 2.1 reduces to the Symplectic Euler algorithm on H_1 (and Algorithm 2.2 reduces to the velocity Verlet algorithm). So, in the limit $\varepsilon \to 0$, the algorithms we have introduced reduce to a symplectic scheme which integrates the limit dynamics.

Additionally, the time step h being fixed, we check that

$$\lim_{\varepsilon\to 0} \frac{P_2^T P_2 + \Omega^2 \ Q_2^T Q_2/(\varepsilon^2)}{p_2^T p_2 + \Omega^2 \ q_2^T q_2/(\varepsilon^2)} = 1$$

for Algorithms 2.1 and 2.2. This is consistent with the fact that $\dfrac{p_2^T p_2}{2} + \Omega^2 \ \dfrac{q_2^T q_2}{2\varepsilon^2}$ is an adiabatic invariant of the dynamics (see [2, 3]).

2.2. **Numerical results.** This section presents some numerical results obtained with Algorithm 2.2 for the integration of (1)-(2) in the case of a constant fast frequency.

The test-bed chosen for our comparison is the commonly used Fermi-Pasta-Ulam spring chain [21, Sec. XIII.2.1]. This chain is a collection of one-dimensional springs, that is fixed at its two end points. The even numbered springs are stiff and harmonic, whereas the odd numbered springs are nonharmonic and nonstiff (see Figure 1). We consider here the case of seven springs, described by six degrees of freedom since the total length of the system is prescribed. In this case, $q_1 = (q_{1,1},q_{1,2},q_{1,3}) \in \mathbb{R}^3$, $q_2 \in \mathbb{R}^3$, $\Omega(q_1) = 1$, and the potential energy V_0 in (1) reads

$$V_0 = \frac{1}{4}\left((q_{1,1}-q_{2,1})^4 + \sum_{i=1}^{2}(q_{1,i+1}-q_{2,i+1}-q_{1,i}-q_{2,i})^4 + (q_{1,3}+q_{2,3})^4\right).$$

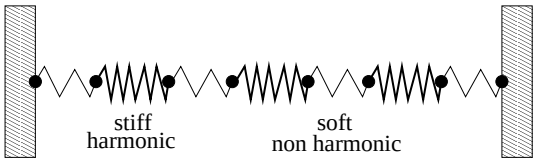

FIGURE 1. Fermi-Pasta-Ulam spring chain.

The energy in the fast spring j $(1 \leq j \leq 3)$ reads $I_j(q,p) = \frac{p_{2,j}^2}{2} + \frac{q_{2,j}^2}{2\varepsilon^2}$ and

$$I(q,p) = I_1(q,p) + I_2(q,p) + I_3(q,p) \tag{18}$$

is an adiabatic invariant in the sense of [21, Theorem XIII.6.3].

In the following, we first study our algorithm regarding the computation of the exact trajectory. Following the practice of [21, Sec. XIII.2], we then compare our algorithm to the exponential integrators proposed in the literature. We name these various algorithms as in [21, Sec. XIII.2] and [14] (see Table 1).

Algorithm	Reference	
A	Gautschi [13]	Non symplectic
B	Deuflhard [8] and Impulse algorithm [15, 34]	Symplectic
C	Garcia-Archilla *et al*, Mollify algorithm [12]	Symplectic
D	Hochbruck and Lubich [19]	Non symplectic
E	Hairer and Lubich [20]	Non symplectic
G	Grimm and Hochbruck [14]	Non symplectic

TABLE 1. Some exponential integrators proposed in the literature. All these integrators are symmetric.

2.2.1. *Long time energy preservation.* As mentioned in the Introduction, we cannot refer to backward error analysis to justify long time energy preservation for the symplectic algorithms proposed above. Indeed, these algorithms are useful in the regime where the time step is large compared to the shortest period present in the system. In the present state of our understanding, all we can do is therefore *test* them, that is numerically check that energy is well-preserved.

We work with $\varepsilon = 0.02$ and $h = 0.17$, and monitor the energy and the adiabatic invariant (18) up to time $T = 10^6$, which is a rather large value compared to final times usually considered with this stiffness. The results obtained with Algorithm 2.2 are shown on Figure 2. No drift can be seen.

2.2.2. *Exchange of fast energies.* The sum $I(q,p)$ of the energies in the fast springs, given by (18), is an adiabatic invariant of the exact trajectory. Exchanges of energy between the fast springs occur on a time scale of order ε^{-1} (see [21, Sec. XIII.2.1]). We study how Algorithm 2.2 reproduces these exchanges.

Following [21, Fig. XIII.2.4], we set $\varepsilon = 0.02$ and $h = 0.03$. Results are shown on Figure 3. The exact trajectory and the numerically computed trajectory satisfactorily agree. We do not include the results for $\varepsilon = 10^{-3}$. They are similar, although the exchanges (for both the exact and the approximated trajectory) are much slower.

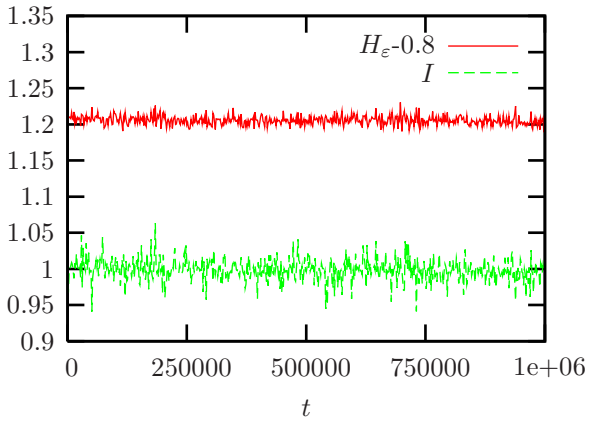

FIGURE 2. Energy (for convenience, we plot $H_\varepsilon - 0.8$) and adiabatic invariant I along the trajectory computed with Algorithm 2.2 ($\varepsilon = 0.02$ and $h = 0.17$).

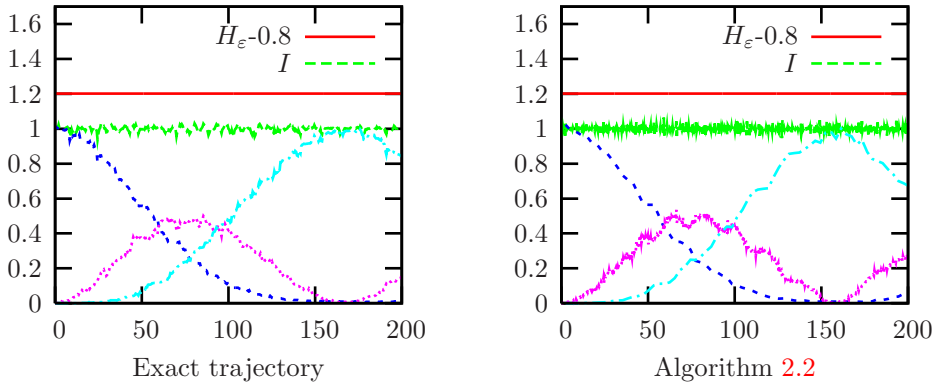

FIGURE 3. Preservation of the energy (for convenience, we plot $H_\varepsilon - 0.8$), of the adiabatic invariant I and exchange between the $\{I_j\}_{1\leq j\leq 3}$ for $\varepsilon = 0.02$ (Algorithm 2.2 has been used with $h = 0.03$).

2.2.3. *Comparison on a test case with a fixed stiffness.* We now set $\varepsilon = 10^{-3}$, and study our algorithm when the time step h varies. We compare Algorithm 2.2 with the exponential integrators described in [21, Chap. XIII] and in [14] (we omit in our comparison the Impulse algorithm (B), since it is usually outperformed by the Mollify algorithm (C); we have checked this in the particular situation considered here).

We first study the preservation of the energy and of the adiabatic invariant. On Figure 4, we plot, as a function of the time step h, the relative error

$$\text{err} = \max_{t\in[0,10^4]} \frac{|H_\varepsilon(t) - H_\varepsilon(0)|}{H_\varepsilon(0)} \tag{19}$$

on the energy conservation over the time interval $[0, 10^4]$. On Figure 5, we plot

$$\max_{t\in[0,10^4]} \frac{|I(t) - I(0)|}{I(0)}, \tag{20}$$

which is the maximum variation to the initial value of the adiabatic invariant (18). On the exact trajectory with $\varepsilon = 10^{-3}$, we observe that this quantity is close to 0.0037.

As is well-known [21, Fig. XIII.2.5], for several exponential integrators, resonances appear when h is a (odd or even or both) multiple of $\varepsilon\pi$, which is half the period of the fast motion. There are almost no resonances with Algorithm 2.2. However, for all the algorithms considered here, these resonances are very peaked: it is easy to find a time step h for which the algorithms are not resonant. We note that Algorithm 2.2 preserves the energy with an equal or better accuracy than all the other algorithms. Algorithms G and 2.2 have no resonances, and the latter preserves the energy with a better accuracy than Algorithm G. We also observe that the adiabatic invariant variation (20) is very well reproduced by Algorithm 2.2.

Remark 3. We work with ε small. Indeed, when we compute an approximation of the generating function, we have made a truncation in the series in powers of ε (see (17)). If ε is too large, this truncation does not make sense. Since ε is small, q_2 is also small, which implies that $V_0(q_1, q_2)$ could be well-approximated by a harmonic function of q_2, a test case that seems less challenging than the one with a function V_0 truly nonharmonic in q_2. However, despite its apparent simplicity, we observe that the test case at hand here is not so easy to deal with, since resonances appear with some of the algorithms.

We next study the global errors at time T, which we define by

$$\text{err} = \|x_{\text{num}}(T) - x_{\text{exact}}(T)\|_2 \tag{21}$$

for a variable $x \in \mathbb{R}^3$, where $\|\cdot\|_2$ is the Euclidean norm in $\mathbb{R}^3$, $x_{\text{exact}}(T)$ is the value of the variable x on the exact trajectory at time T and $x_{\text{num}}(T)$ is its approximation on the numerically computed trajectory. Following [14, Fig. 2], we study these errors at time $T = 1$, for the variable $x \equiv q_1$, $x \equiv q_2/\varepsilon$ (which is of order $O(1)$ in ε), $x \equiv p_1$ and $x \equiv p_2$. Results are shown on Figure 6. For the slow variables q_1 and p_1, we have gathered exponential algorithms for which the error was almost the same. For the fast variables q_2/ε and p_2, we have kept the two exponential algorithms that provide the smallest errors (see [14, Fig. 2] and [21, Fig. XIII.2.2] for more comprehensive numerical results).

We first see that, with Algorithm 2.2, the error does not converge to 0 when $h \to 0$. This is due to the truncation in the series in powers of ε performed to approximate the generating function. Even if $h \to 0$, an error remains. Note however that we are not interested in the regime $h \to 0$, for numerical efficiency reasons.

As soon as $h \geq \varepsilon\pi$, we observe that the error on the slow variables q_1 and p_1 is similar for Algorithm 2.2 and for the exponential integrators A, C, D, E and G, provided we use a non-resonant time step for the latter algorithms. We now turn to the fast variables. In the regime $h \geq \varepsilon\pi$ of practical interest, the error with Algorithm 2.2 is much smaller than the error with the exponential integrators. There is no resonance with Algorithm 2.2. In summary, we observe a good accuracy on the solution at time $T = 1 \gg \varepsilon$ computed with Algorithm 2.2 proposed here. Note that this time T is much longer than the time scale ε of the fast variables.

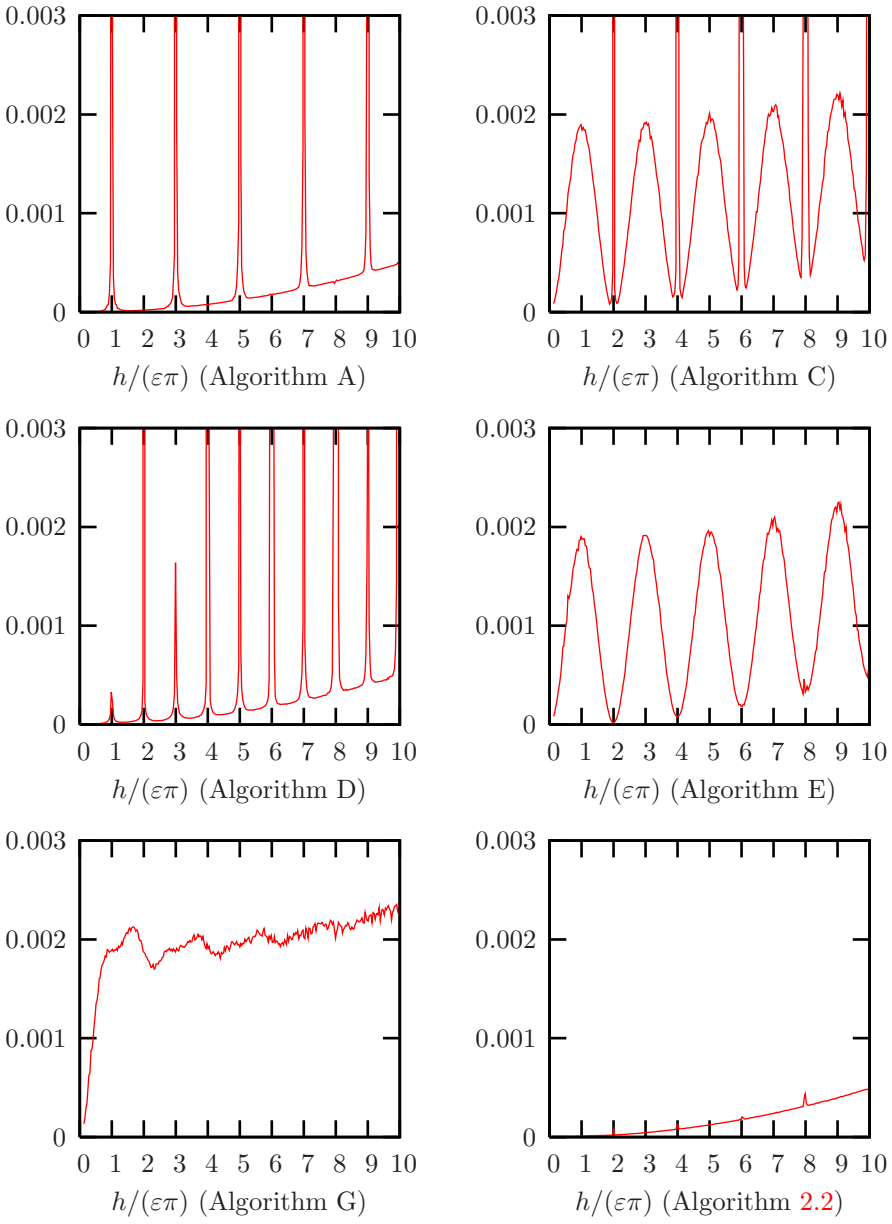

FIGURE 4. Maximum relative variation (19) of the energy on the time interval $[0, 10^4]$, for several time steps h ($\varepsilon = 10^{-3}$). See Table 1 for exponential algorithms terminology.

We next set $\varepsilon = 0.02$, and monitor again the energy and adiabatic invariant preservations, with the estimators (19) and (20), on the time interval $[0, 10^4]$. On the exact trajectory with $\varepsilon = 0.02$, the estimator (20) is close to 0.093. Numerical results are shown on Figures 7 and 8. We observe that all integrators uniformly perform less well than in the case $\varepsilon = 10^{-3}$. Indeed, when increasing ε while

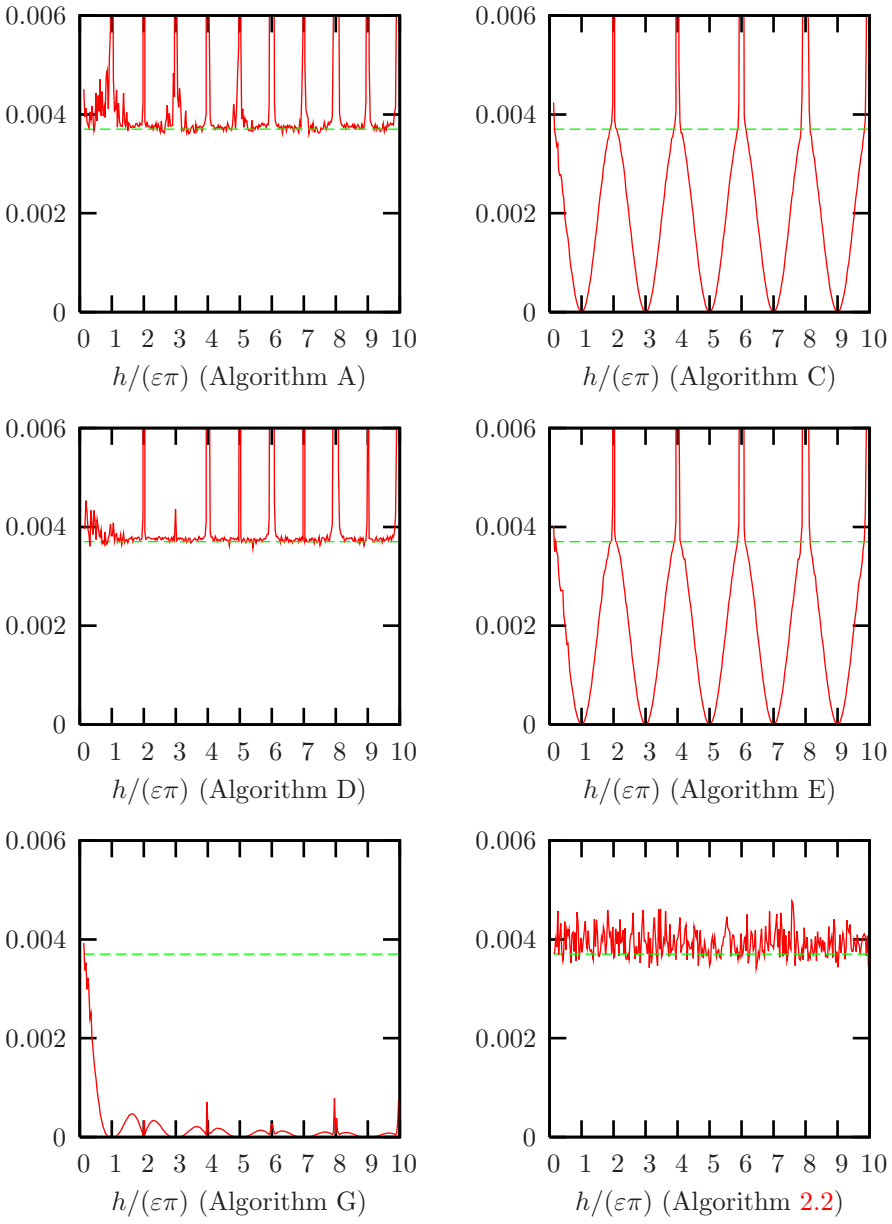

FIGURE 5. Maximum variation (20) of the adiabatic invariant on the time interval $[0, 10^4]$, for several time steps h ($\varepsilon = 10^{-3}$). We compare the numerical results with the exact result, which is here 0.0037 (see body of the text). See Table 1 for exponential algorithms terminology.

keeping $h/(\varepsilon\pi)$ constant, h increases and thus the slow dynamics is integrated less accurately. We observe that the algorithm 2.2, despite being built for the regime of small ε, again gives better results than the other algorithms of the literature, when $\varepsilon = 0.02$ and $h \leq 0.2$ (that is, $h/(\varepsilon\pi) \leq 3$).

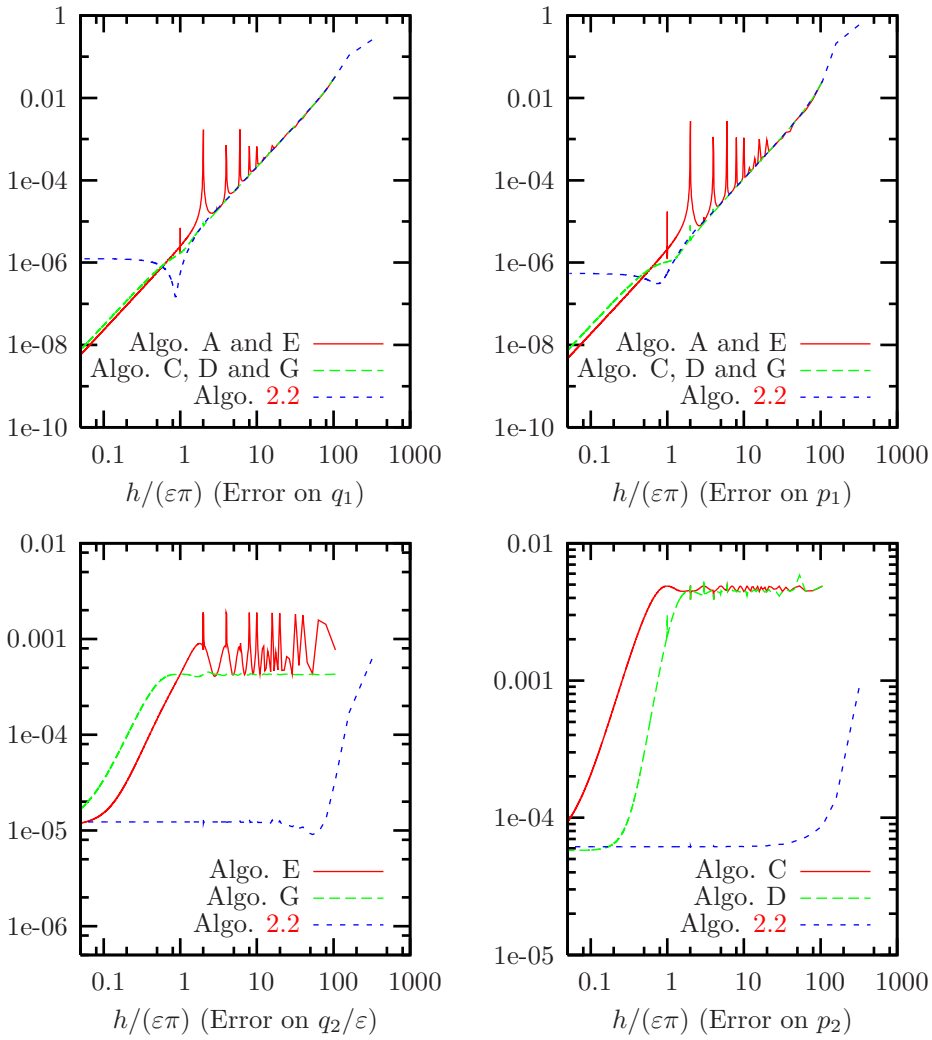

FIGURE 6. Global errors (21) at time $T = 1$, for several time steps h ($\varepsilon = 10^{-3}$). For the fast variables, only the results for the exponential integrators that best perform are shown. See Table 1 for exponential algorithms terminology.

Let us emphasize that the conclusions drawn from the comparison between the algorithm 2.2 developed in the present work and the algorithms C, D and E are limited to the specific context considered. The algorithms C, D and E can be used for *any* Hamiltonian system with a slow/fast potential energy separation, whereas the algorithms introduced here apply to Hamiltonians of the form (1). On the other hand, and this is then a fair comparison, Algorithm 2.2 outperforms the integrators A and G, specifically developed for (1).

2.2.4. *Robustness of the algorithms.* Let us now compare the algorithms using a fixed time step $h = 0.02$, and a varying stiffness. Our aim is to check that the errors in the energy and adiabatic invariant preservations do not depend on ε, and

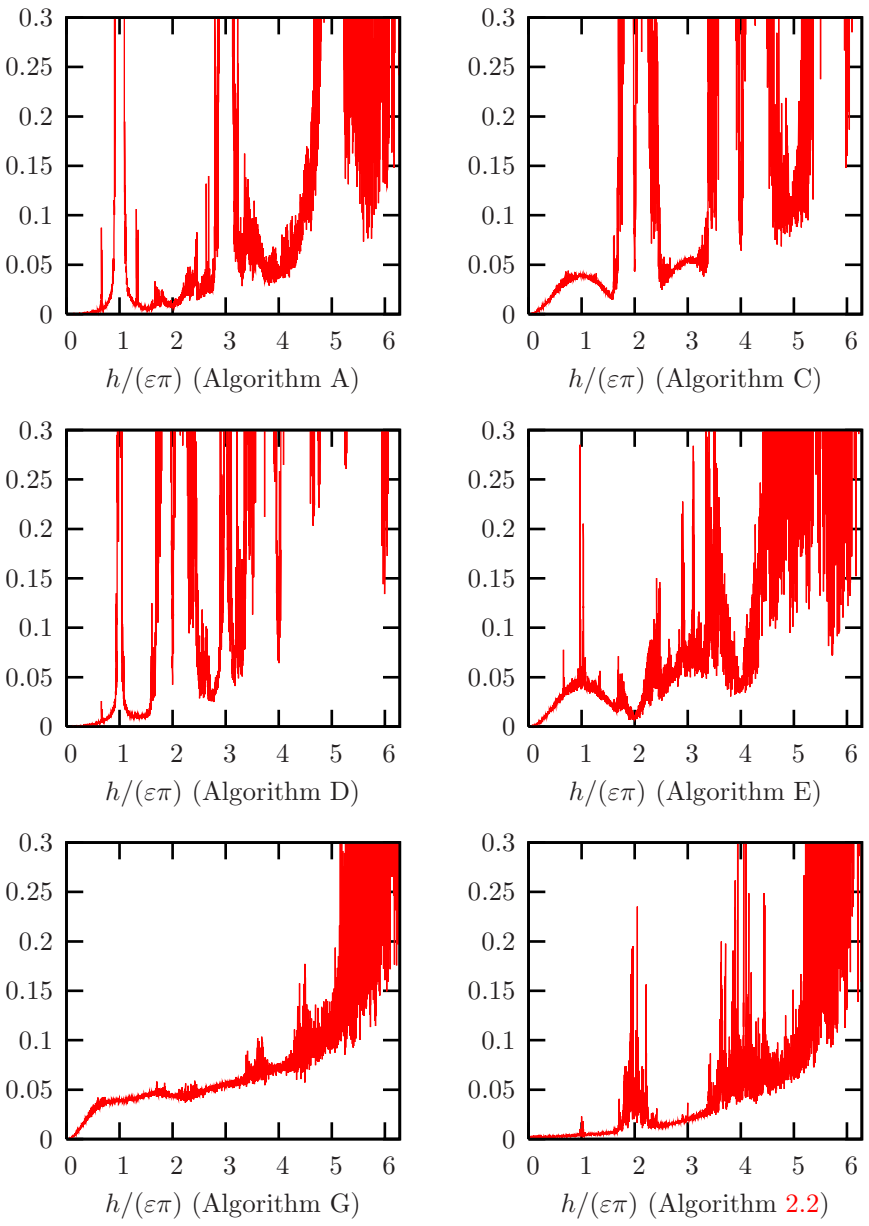

FIGURE 7. Maximum relative variation (19) of the energy on the time interval $[0, 10^4]$, for several time steps h ($\varepsilon = 0.02$). See Table 1 for exponential algorithms terminology.

thus that we can use a time step h which is not bounded by ε, as would be the case for a standard algorithm (such as velocity-Verlet).

We again use the estimators (19) and (20). Results are shown on Figures 9 and 10. We again see that ε has to be sufficiently small for the energy to be well-preserved by Algorithm 2.2. When ε is sufficiently small, we observe that the

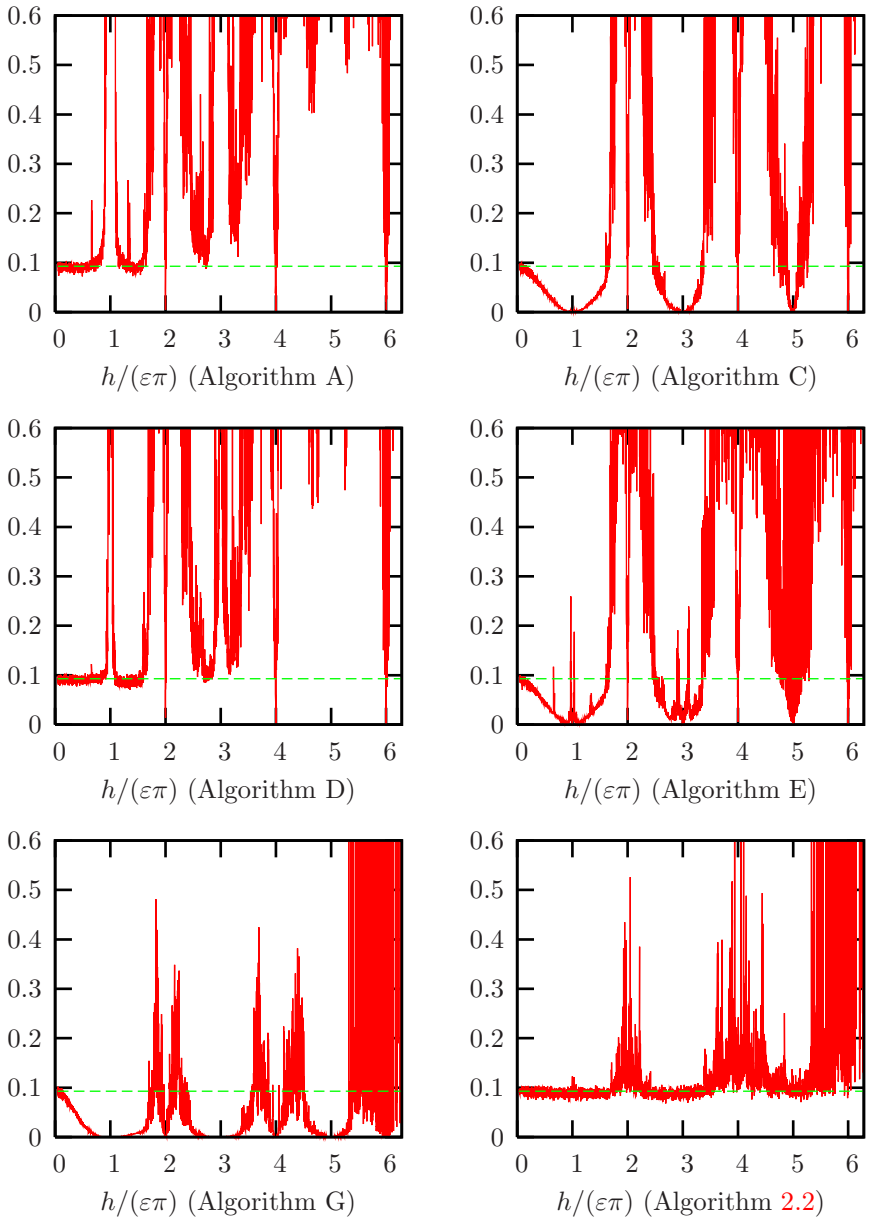

FIGURE 8. Maximum variation (20) of the adiabatic invariant on the time interval $[0, 10^4]$, for several time steps h ($\varepsilon = 0.02$). We compare the numerical results with the exact result, which is here 0.093. See Table 1 for exponential algorithms terminology.

accuracy in the energy preservation does not depend on ε, so the algorithms are unsensitive to the stiffness, up to the occurence of resonances. The variations of the adiabatic invariant, that become larger when ε increases, are very well reproduced by Algorithm 2.2.

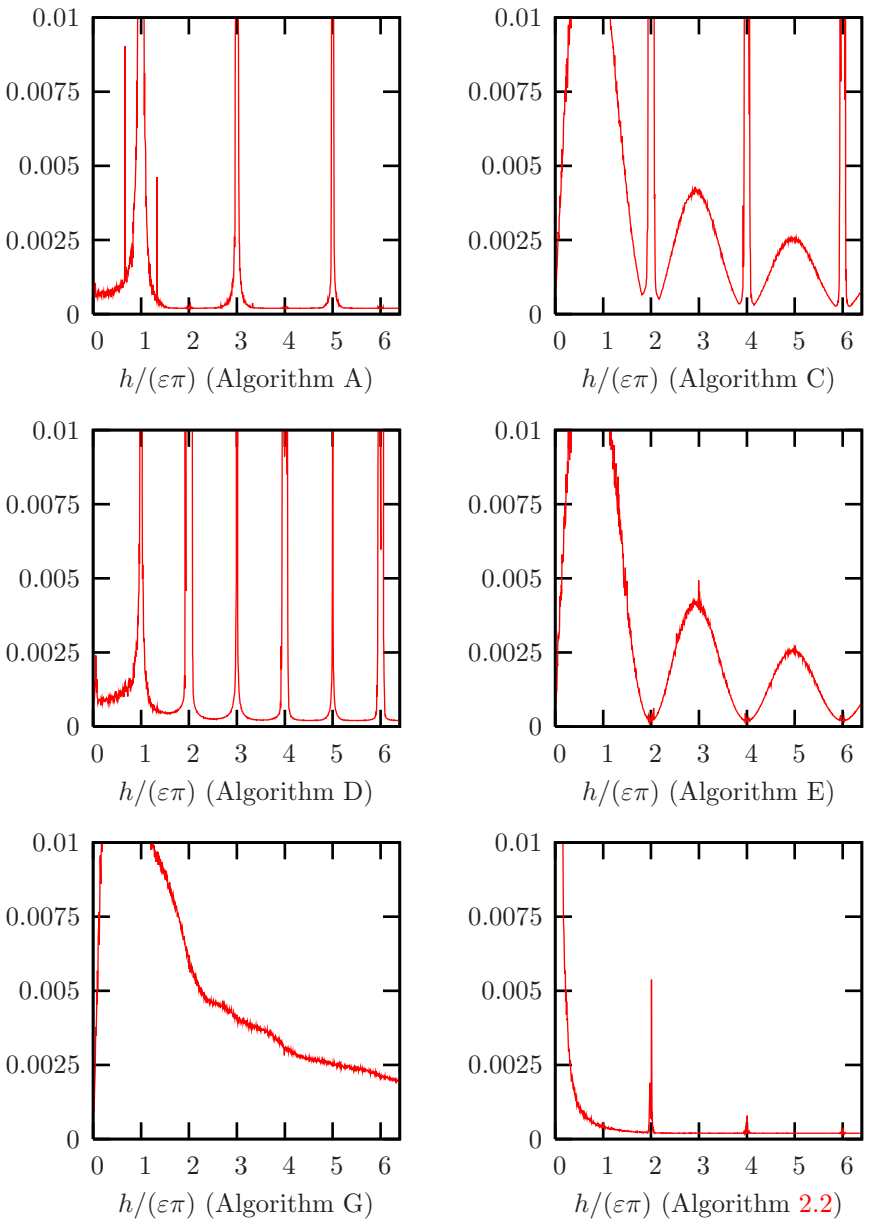

FIGURE 9. Maximum relative variation (19) of the energy on the time interval $[0, 10^4]$, for several ε ($h = 0.02$). See Table 1 for exponential algorithms terminology.

3. **Non constant fast frequency.** We now consider the case when the fast frequency $\Omega(q_1)$ actually depends on q_1. In Section 3.1, we derive an efficient symplectic algorithm. For brevity, we focus on the differences between the present case and the case of a constant frequency. We report on numerical tests in Section 3.2.

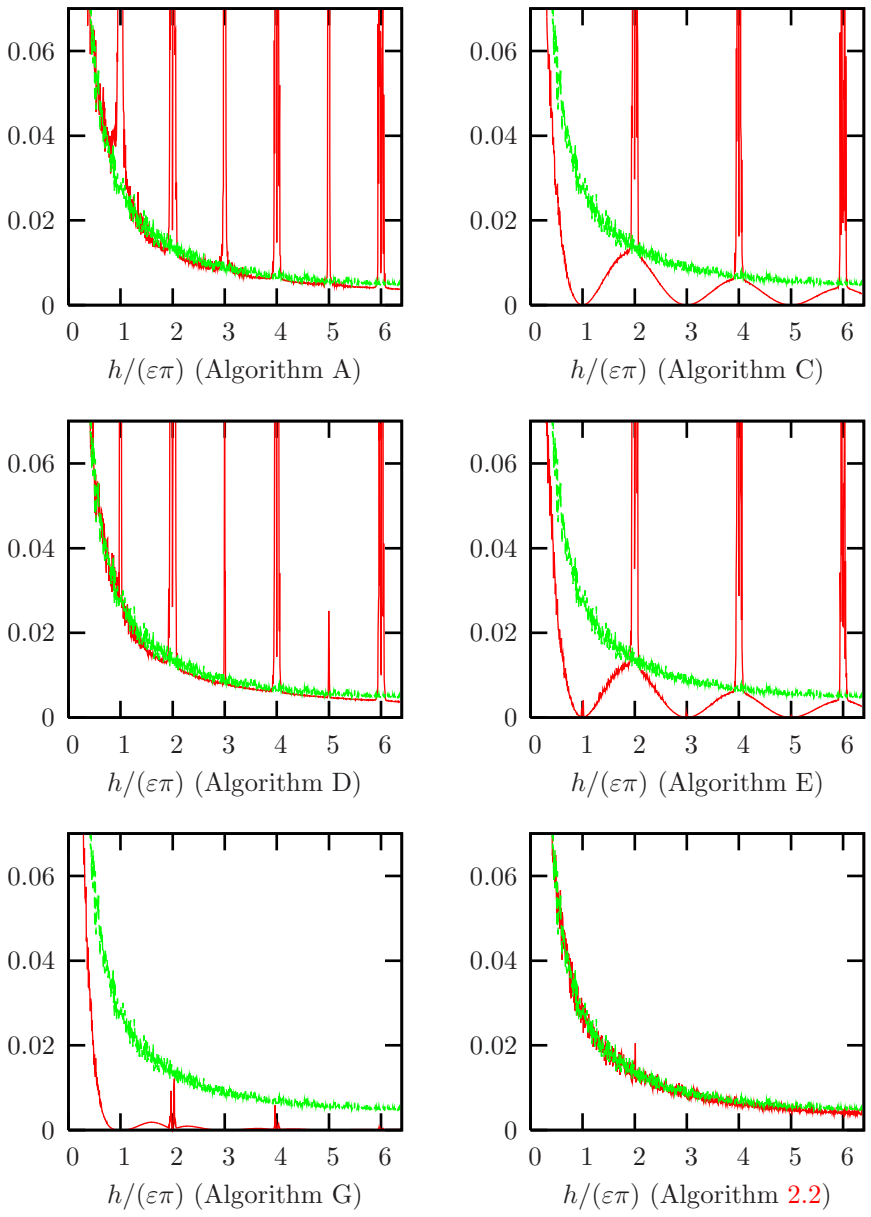

FIGURE 10. Maximum variation (20) of the adiabatic invariant on the time interval $[0, 10^4]$, for several ε ($h = 0.02$). We compare the numerical results (red curve) with the exact result (green curve). See Table 1 for exponential algorithms terminology.

At the beginning of Section 2, we have underlined that (at least) two variants are possible in the case of a constant frequency. In this section, we only follow the first strategy, namely the one which consists in working with the original variables. It is

not yet clear to us whether the second strategy mentioned earlier can be adapted to the case of a non constant frequency.

3.1. **Derivation of a symplectic algorithm.** We consider the following Ansatz

$$\begin{aligned} S_\varepsilon(t,q_1,r_2,P_1,P_2) &= S_0(t,q_1,P_1) \\ &+ \sum_{k\geq 1}\varepsilon^k S_k\left(t,\frac{T(t,q_1,P_1)}{\varepsilon},q_1,r_2,P_1,P_2\right) \end{aligned} \tag{22}$$

for the solution to (6)-(7), where $(S_k)_{k\geq 1}$ are 2π periodic functions in the fast time $\tau = T(t,q_1,P_1)/\varepsilon$. The fast time is chosen such that $\partial_t T = \Omega(q_1(t))$, hence

$$T = \int_0^t \Omega(q_1(s))\,ds.$$

We need to approximate this equation so that T only depends on t, q_1 and P_1. A trapezoidal approximation reads

$$\begin{aligned} T(t) &= \frac{t}{2}\left[\Omega(q_1(0)) + \Omega(q_1(t))\right] + O(t^3) \\ &= \frac{t}{2}\left[\Omega(q_1(0)) + \Omega\left(q_1(0) + \frac{\partial S_0}{\partial P_1}\right)\right] + O(t^3) + O(\varepsilon t) \\ &= \frac{t}{2}\left[\Omega(q_1) + \Omega\left(q_1 + t\frac{\partial^2 S_0}{\partial P_1 \partial t}(t=0)\right)\right] + O(t^3) + O(\varepsilon t). \end{aligned}$$

We set

$$T(t,q_1,P_1) := \frac{t}{2}\left[\Omega(q_1) + \Omega\left(q_1 + t\frac{\partial^2 S_0}{\partial P_1 \partial t}(t=0)\right)\right] \tag{23}$$

and

$$\tau = \frac{T(t,q_1,P_1)}{\varepsilon}, \tag{24}$$

which is an approximation of order $O(t^3/\varepsilon) + O(t)$ of the exact phase. Thus, if $t \ll \varepsilon^{1/3}$, then τ is a good approximation of the exact phase.

We now insert (22) in (6)-(7), and compare like-powers of ε. For instance, the equation of order ε^0 reads

$$\begin{aligned} \partial_t S_0 + \partial_t T\,\partial_\tau S_1 &= \frac{P_1^T P_1}{2} + \frac{P_2^T P_2}{2} + V_0(q_1 + \partial_{P_1} S_0, 0) \\ &+ \frac{1}{2}\Omega(q_1 + \partial_{P_1} S_0)^2 \left(\frac{r_2}{\Omega(q_1)} + \partial_{P_2} S_1\right)^T \left(\frac{r_2}{\Omega(q_1)} + \partial_{P_2} S_1\right), \end{aligned}$$

that we next expand in powers of t. After some tedious but not difficult computations (see [28] for details), we obtain

$$\begin{aligned} S_0(t=0) &= 0, \\ \partial_t S_0(t=0) &= \frac{P_1^T P_1}{2} + V_0(q_1,0), \\ S_1(t=0) &= \frac{1}{\Omega(q_1)}\left(\frac{P_2^T P_2 + r_2^T r_2}{2}\right)\tan\tau + \frac{P_2^T r_2}{\Omega(q_1)}\left(\frac{1}{\cos\tau} - 1\right), \\ \partial_{tt} S_0(t=0) &= P_1^T \nabla_1 V_0(q_1,0), \\ \partial_t S_1(t=0) &= -\frac{P_1^T \nabla\Omega(q_1)}{\Omega^2(q_1)}\left(\frac{r_2^T P_2}{2\cos\tau} + \frac{P_2^T P_2 \tan\tau}{2}\right), \end{aligned} \tag{25}$$

where all functions S_k and their derivatives are evaluated at $(t=0,\tau,q_1,r_2,P_1,P_2)$.

We first consider the approximation $S_\varepsilon(h) \approx \widetilde{S_\varepsilon}(h)$, with

$$\boxed{\widetilde{S_\varepsilon}(h) := S_0 + h\partial_t S_0 + \varepsilon S_1 + \varepsilon h \partial_t S_1.} \tag{26}$$

The scheme on the fast variables is obtained from (5), and reads

$$P_2 = \frac{(\cos\tau)p_2 - (\sin\tau)r_2}{1-\beta/2}, \tag{27}$$

$$Q_2 = \frac{\varepsilon}{\Omega}\tan\tau\,(1-\beta)\,P_2 + \frac{1}{\cos\tau}\left(1-\frac{\beta}{2}\right)q_2, \tag{28}$$

with

$$\beta = \frac{h}{\Omega(q_1)} P_1^T \nabla\Omega(q_1).$$

When $\cos\tau \to 0$ and $\sin\tau \to 1$, we can approximate (28) by

$$Q_2 \approx \frac{1}{(\cos\tau)(1-\beta/2)}\,\frac{\beta^2}{4}\,q_2.$$

So the scheme is singular in the limit $\cos\tau \to 0$. To remove this singularity, we slightly modify the generating function. We have

$$\begin{aligned}\widetilde{S_\varepsilon}(h) = \quad & h\left(\frac{1}{2}P_1^T P_1 + V_0(q_1,0)\right) \\ & + \frac{\varepsilon}{\Omega(q_1)}\left[\frac{r_2^T r_2}{2}\tan\tau + \frac{P_2^T P_2}{2}(1-\beta)\tan\tau - r_2^T P_2 + \frac{r_2^T P_2}{\cos\tau}\left(1-\frac{\beta}{2}\right)\right],\end{aligned}$$

that we replace by

$$\boxed{\begin{aligned}S_\varepsilon^{\rm NC}(h) := \quad & h\left(\frac{1}{2}P_1^T P_1 + V_0(q_1,0)\right) + \frac{\varepsilon}{\Omega(q_1)}\left[\frac{r_2^T r_2}{2}\tan\tau\right. \\ & \left. + \frac{P_2^T P_2}{2}\exp(-\beta)\tan\tau - r_2^T P_2 + \frac{r_2^T P_2}{\cos\tau}\exp(-\beta/2)\right].\end{aligned}} \tag{29}$$

The difference between (29) and (26) is of order $O(h^2\varepsilon)$, so the order of the approximation has not been modified.

In view of (23), (24) and (25), the fast time τ reads

$$\tau = \frac{h}{2\varepsilon}\left[\Omega(q_1) + \Omega(q_1 + hP_1)\right]. \tag{30}$$

We now insert $S_\varepsilon^{\rm NC}(h)$ into (5), and obtain the scheme $\Psi_h^{\rm NC}$ (see Algorithm 3.1), which is well defined even in the limit $\cos\tau \to 0$ (see in particular Steps 4 and 5 of the algorithm, that replace (27) and (28)). This scheme is symplectic. The new momentum P_1 is implicitly defined (see Step 2 of the algorithm; note in particular that the fast time τ depends on P_1, in view of (30)). Once P_1 is determined, the other variables Q_1, Q_2 and P_2 can be computed in an explicit fashion. Computing P_1 amounts to solving a nonlinear equation of the form $\mathcal{F}(P_1) = 0$. To this end, we use a Newton algorithm, and compute the derivative of $\mathcal{F}$ with a finite difference scheme. On the test case reported below, only three iterations were sufficient to converge.

Algorithm 3.1 (Symplectic Scheme $\Psi_h^{\mathrm{NC}}(q_1,q_2,p_1,p_2)$)**.** Set $(q_1,q_2,p_1,p_2) = (q_1^n,q_2^n,p_1^n,p_2^n)$ and perform the following steps:

1. Set $r_2 = \dfrac{\Omega(q_1)}{\varepsilon} q_2$.
2. Solve for P_1 the following implicit equation:

$$\begin{aligned} p_1 = \quad & P_1 + h\nabla_1 V_0(q_1,0) \\ & -\frac{\varepsilon}{\Omega^2(q_1)}\left(p_2^T r_2 \sin^2\tau^* + \frac{r_2^T r_2 - p_2^T p_2}{2}\,\sin\tau^*\cos\tau^*\right)\nabla\Omega(q_1) \\ & +\frac{h}{4\Omega(q_1)}\left(r_2^T r_2 + p_2^T p_2\right)\left(\nabla\Omega(q_1) + \nabla\Omega(q_1+hP_1)\right) \\ & -\frac{h\varepsilon}{\Omega(q_1)}\left[\frac{p_2^T p_2 - r_2^T r_2}{2}\,\sin\tau^*\cos\tau^* + p_2^T r_2\left(\frac{1}{2} - \sin^2\tau^*\right)\right] d(q_1,P_1), \end{aligned}$$

   with $\tau^* = \dfrac{h}{2\varepsilon}\left[\Omega(q_1) + \Omega(q_1+hP_1)\right]$ and $d(q_1,P_1) = \nabla_{q_1}\left(\dfrac{P_1^T\nabla\Omega(q_1)}{\Omega(q_1)}\right)$.
3. Set $\tau = \dfrac{h}{2\varepsilon}\left[\Omega(q_1) + \Omega(q_1+hP_1)\right]$ and $\beta = \dfrac{h}{\Omega(q_1)} P_1^T\nabla\Omega(q_1)$.
4. Set $P_2 = \exp(\beta/2)\left((\cos\tau)p_2 - (\sin\tau)r_2\right)$.
5. Set $Q_2 = \exp(-\beta/2)\left((\cos\tau)q_2 + \dfrac{\varepsilon\sin\tau}{\Omega(q_1)}p_2\right)$.
6. Set

$$\begin{aligned} Q_1 = \quad & q_1 + hP_1 + \frac{h^2}{4\Omega(q_1)}\left(r_2^T r_2 + p_2^T p_2\right)\nabla\Omega(q_1+hP_1) \\ & -\frac{h\varepsilon}{\Omega^2(q_1)}\left[\frac{p_2^T p_2 - r_2^T r_2}{2}\,\sin\tau\cos\tau + p_2^T r_2\left(\frac{1}{2} - \sin^2\tau\right)\right]\nabla\Omega(q_1). \end{aligned}$$

Set $\left(q_1^{n+1},q_2^{n+1},p_1^{n+1},p_2^{n+1}\right) = (Q_1,Q_2,P_1,P_2)$.

Remark 4. In the case of scalar fast variables ($q_2 \in \mathbb{R}$, $p_2 \in \mathbb{R}$), it is shown in [2, 3] that the dynamics on the slow variables obtained in the limit $\varepsilon \to 0$ is a dynamics of Hamiltonian $H_1^{\mathrm{hom}}(q_1,p_1) = \dfrac{p_1^T p_1}{2} + V_0(q_1,0) + C\Omega(q_1)$, where

$$C = \lim_{\varepsilon\to 0} \quad \frac{p_2^2(0) + \Omega^2(q_1(0))\; q_2^2(0)/(\varepsilon^2)}{2\Omega(q_1(0))}$$

is a constant which depends on the initial conditions. We show in this remark that, in the limit $\varepsilon \to 0$, Algorithm 3.1 is consistent with this theoretical result.

We first check that, for the slow variables, in the limit $\varepsilon \to 0$, Algorithm 3.1 is the symplectic algorithm which is derived from the generating function

$$S_{\mathrm{num}}^{\mathrm{hom}}(h,q_1,P_1) = h\left(V_0(q_1,0) + \frac{P_1^T P_1}{2} + \frac{C}{2}\left[\Omega(q_1) + \Omega(q_1+hP_1)\right]\right),$$

where $C = \dfrac{p_2^T p_2 + \Omega^2(q_1)\; q_2^T q_2/(\varepsilon^2)}{2\Omega(q_1)}$ is supposed to be a constant. We observe that $S_{\mathrm{num}}^{\mathrm{hom}}(h,q_1,P_1) = S^{\mathrm{hom}}(h,q_1,P_1) + O(h^2)$, where $S^{\mathrm{hom}}(t,q_1,P_1)$ is the solution of the Hamilton-Jacobi equation associated to H_1^{hom}.

In addition, the time step h being fixed, we check on Algorithm 3.1 that

$$\lim_{\varepsilon\to 0} \frac{P_2^T P_2 + \Omega^2(Q_1)\; Q_2^T Q_2/(\varepsilon^2)}{p_2^T p_2 + \Omega^2(q_1)\; q_2^T q_2/(\varepsilon^2)}\;\frac{\Omega(q_1)}{\Omega(Q_1)} = 1 + O(h^2).$$

Up to the term $O(h^2)$, this is consistent with the fact that

$$\frac{1}{\Omega(q_1)}\left(\frac{p_2^T p_2}{2} + \Omega^2(q_1)\,\frac{q_2^T q_2}{2\varepsilon^2}\right)$$

is an adiabatic invariant of the dynamics.

3.2. **Numerical results.** We have implemented Algorithm 3.1 in the scalar case ($q_1 \in \mathbb{R}$, $q_2 \in \mathbb{R}$), with

$$\Omega(q_1) = \sqrt{1+q_1^2} \quad \text{and} \quad V_0(q_1,q_2) = (q_1^2+q_2^2-1)^2.$$

In addition to the preservation of energy, we monitor the variation of

$$I = \frac{\frac{p_2^2}{2} + \Omega(q_1)^2\,\frac{q_2^2}{2\varepsilon^2}}{\Omega(q_1)} \tag{31}$$

along the trajectory. Recall that I is an adiabatic invariant (see [2, 3]), and that, on a given time window, its variation decreases as ε decreases.

We first choose $\varepsilon = 10^{-3}$ and $h = 0.02$, and monitor the evolution of the energy and adiabatic invariant up to time $T = 10^6$. Results are shown on Figure 11. No drift can be seen.

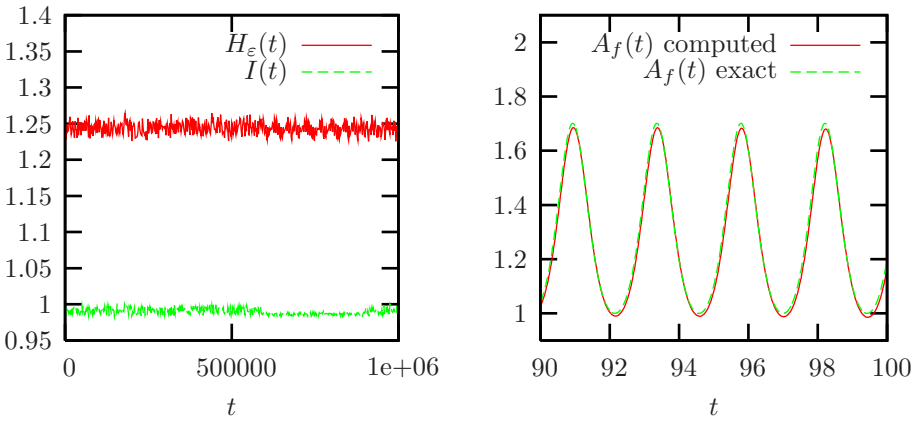

FIGURE 11. Left: Energy and adiabatic invariant along the trajectory computed with Algorithm 3.1 ($\varepsilon = 10^{-3}$ and $h = 0.02$). Right: as expected, $A_f = \frac{p_2^2}{2} + (\Omega(q_1))^2\,\frac{q_2^2}{2\varepsilon^2}$ varies.

We now let the time step h vary, while keeping the stiffness at its prescribed value $\varepsilon = 10^{-3}$. On Figure 12, we plot the variation of the energy (see estimator (19)) and the variation of the adiabatic invariant (31) (see estimator (20)), over the time interval $t \in [0, 10^4]$. We observe a good behaviour of the algorithm: even if h is much larger than ε, the energy and the adiabatic invariant are preserved with a good accuracy (the error is less than 1% for all $h \leq 10\varepsilon$). For $h \leq 10\varepsilon$, the variation of the energy seems to be proportional to h, up to very peaked resonances. This behaviour is consistent with the approximation (26)-(29), where terms of order h^2 have been neglected.

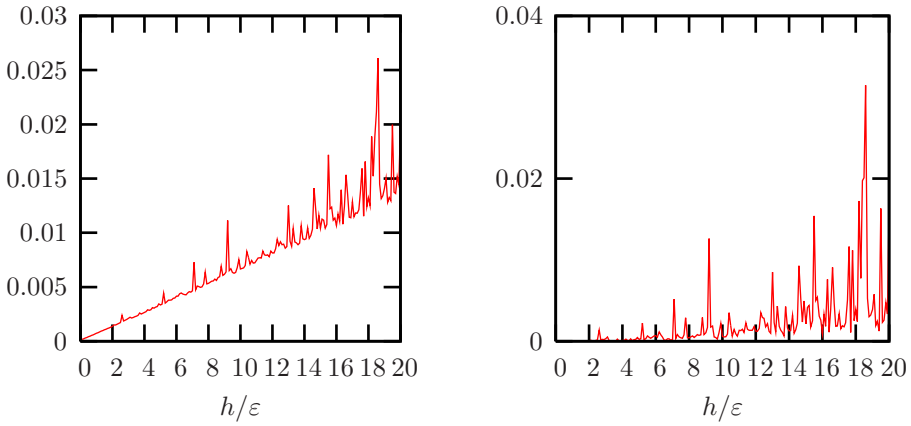

FIGURE 12. Maximum variation (19) of the energy (left) and maximum variation (20) of the adiabatic invariant (right) on the time interval $[0, 10^4]$, for several h ($\varepsilon = 10^{-3}$), for Algorithm 3.1.

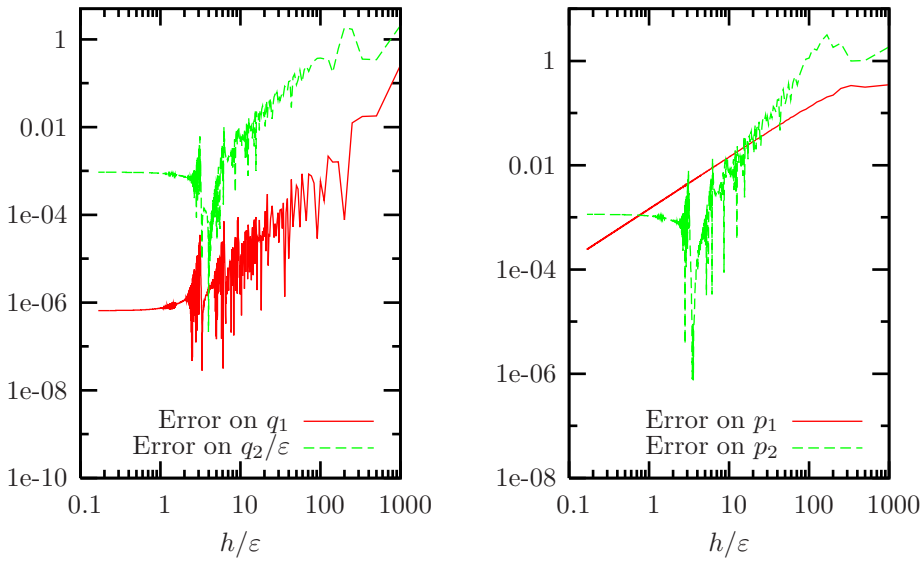

FIGURE 13. Global errors (21) at time $T = 1$, for several time steps h ($\varepsilon = 10^{-3}$).

On Figure 13, we plot the global errors (21) at time $T = 1$ of q_1, q_2/ε, p_1 and p_2. We again observe a very good accuracy, even if $h \gg \varepsilon$.

We finally study the robustness of the algorithm. We set the time step to $h = 0.02$, and consider the variation of the energy and of the adiabatic invariant, over the time interval $t \in [0, 10^4]$, for stiffness ε varying between 10^{-3} to 1. Results are shown on Figure 14. When ε decreases to 0, the algorithm performs equally well, up to peaked resonances.

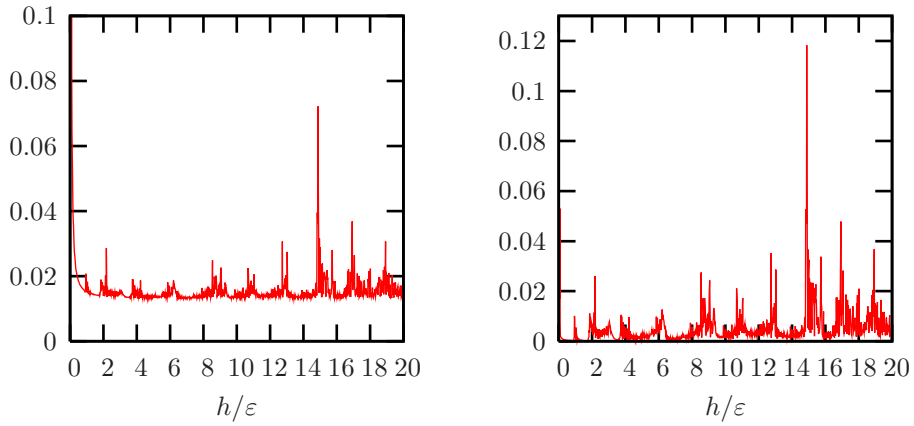

FIGURE 14. Maximum variation (19) of the energy (left) and maximum variation (20) of the adiabatic invariant (right) on the time interval $[0, 10^4]$, for several ε ($h = 0.02$), for Algorithm 3.1.

Acknowledgments. This work is supported in part by the INGEMOL and MEGAS non-thematic programs (Agence Nationale de la Recherche, France), by the Action Concertée Incitative "Nouvelles Interfaces des Mathématiques" SIMUMOL (Ministère de la Recherche et des Nouvelles Technologies) and by the INRIA, under the grant "Action de Recherche Collaborative" HYBRID. The authors thank Philippe Chartier, Ernst Hairer and Christian Lubich for stimulating discussions. The second author wishes to acknowledge the hospitality of the Isaac Newton Institute (Cambridge, UK). Constructive comments of the anonymous referees greatly improved the manuscript.

REFERENCES

[1] G. Benettin and A. Giorgilli, *On the Hamiltonian interpolation of near to the identity symplectic mappings with application to symplectic integration algorithms*, J. Stat. Phys., **74** (1994), 1117–1143.

[2] F. Bornemann, "Homogenization in Time of Singularly Perturbed Mechanical Systems," Lecture Notes in Mathematics, no. 1687, Springer, Berlin, 1998.

[3] F. Bornemann and Ch. Schuette, *Homogenization of Hamiltonian systems with a strong constraining potential*, Physica D, **102** (1997), 57–77.

[4] F. Castella, Ph. Chartier and E. Faou, *An averaging technique for highly-oscillatory Hamiltonian problems*, SIAM J. Numer. Anal., **47** (2009), 2808–2837.

[5] D. Cohen, E. Hairer and Ch. Lubich, *Modulated Fourier expansions of highly oscillatory differential equations*, Found. Comput. Math., **3** (2003), 327–345.

[6] ———, *Numerical energy conservation for multi-frequency oscillatory differential equations*, BIT, **45** (2005), 287–305.

[7] D. Cohen, T. Jahnke, K. Lorenz and Ch. Lubich, *Numerical integrators for highly oscillatory Hamiltonian systems: A review*, Analysis, Modeling and Simulation of Multiscale Problems (A. Mielke, ed.), Mathematics and Statistics, Springer, 2006, 553–576.

[8] P. Deuflhard, *A study of extrapolation methods based on multistep schemes without parasitic solutions*, Z. Angew. Math. Phys., **30** (1979), 177–189.

[9] B. Engquist and R. Tsai, *Heterogeneous multiscale methods for stiff ordinary differential equations*, Math. Comput., **74** (2005), 1707–1742.

[10] K. Feng, *Difference schemes for Hamiltonian formalism and symplectic geometry*, J. Comp. Math., **4** (1986), 279–289.

[11] E. Faou, E. Hairer and T.-L. Pham, *Energy conservation with non-symplectic methods: examples and counter-examples*, BIT, **44** (2004), 699–709.
[12] B. Garcia-Archilla, J. M. Sanz-Serna and R. D. Skeel, *Long time step methods for oscillatory differential equations*, SIAM J. Sci. Comput., **20** (1999), 930–963.
[13] W. Gautschi, *Numerical integration of ordinary differential equations based on trigonometric polynomials*, Numer. Math., **3** (1961), 381–397.
[14] V. Grimm and M. Hochbruck, *Error analysis of exponential integrators for oscillatory second-order differential equations*, J. Phys. A, **39** (2006), 5495–5507.
[15] H. Grubmüller, H. Heller, A. Windemuth and K. Schulten, *Generalized Verlet algorithm for efficient molecular dynamics simulations with long range interaction*, Mol. Sim., **6** (1991), 121–142.
[16] E. Hairer, *Long time energy conservation of numerical integrators*, Foundations of Computational Mathematics, Santander 2005, London Math. Soc. Lecture Notes, vol. **331**, Cambridge University Press, 2006, 162–180.
[17] E. Hairer and Ch. Lubich, *The life-span of backward error analysis for numerical integrators*, Numer. Math., **76** (1997), 441–462, Erratum: http://www.unige.ch/math/folks/hairer.
[18] ———, *Energy conservation by Störmer-type numerical integrators*, Numerical Analysis (D. F. Griffiths and G. A. Watson, eds.), CRC Press LLC, 1999, 169–190.
[19] M. Hochbruck and Ch. Lubich, *A Gautschi-type method for oscillatory second-order differential equations*, Numer. Math., **83** (1999), 403–426.
[20] E. Hairer and Ch. Lubich, *Long-time energy conservation of numerical methods for oscillatory differential equations*, SIAM J. Numer. Anal., **38** (2000), 414–441.
[21] E. Hairer, Ch. Lubich and G. Wanner, "Geometric Numerical Integration," Structure-preserving algorithms for ordinary differential equations, Second edition. Springer Series in Computational Mathematics, 31, Springer-Verlag, Berlin, 2006.
[22] J. A. Izaguirre, S. Reich and R. D. Skeel, *Longer time steps for molecular dynamics*, J. Chem. Phys., **110** (1999), 9853–9864.
[23] A. Iserles, *On the global error of discretization methods for highly-oscillatory ordinary differential equations*, BIT, **42** (2002), 561–599.
[24] T. Jahnke, *Long-time-step integrators for almost-adiabatic quantum dynamics*, SIAM J. Sci. Comput., **25** (2004), 2145–2164 (electronic).
[25] T. Jahnke and Ch. Lubich, *Numerical integrators for quantum dynamics close to the adiabatic limit*, Numer. Math., **94** (2003), 289–314.
[26] Z. Jia and B. Leimkuhler, *Geometric integrators for multiple time-scale simulation*, J. Phys. A, **39** (2006), 5379–5403.
[27] C. Le Bris and F. Legoll, *Dérivation de schémas numériques symplectiques pour des systèmes hamiltoniens hautement oscillants (derivation of symplectic numerical schemes for highly oscillatory Hamiltonian systems)*, C. R. Acad. Sci. Paris, Série I, **344** (2007), 277–282.
[28] ———, *Integrators for highly oscillatory Hamiltonian systems: An homogenization approach*, Tech. Report 6252, INRIA, july 2007, http://hal.inria.fr/inria-00165293/en.
[29] K. Lorenz, T. Jahnke and Ch. Lubich, *Adiabatic integrators for highly oscillatory second order linear differential equations with time-varying eigendecomposition*, BIT, **45** (2005), 91–115.
[30] B. J. Leimkuhler and S. Reich, *A reversible averaging integrator for multiple time-scale dynamics*, J. Comput. Phys., **171** (2001), 95–114.
[31] S. Reich, *Backward error analysis for numerical integrators*, SIAM J. Numer. Anal., **36** (1999), 1549–1570.
[32] J. M. Sanz-Serna, *Mollified impulse methods for highly oscillatory differential equations*, SIAM J. Numer. Anal., **46** (2008), 1040–1059.
[33] R. Sharp, R. Tsai and B. Engquist, *Multiple time scale numerical methods for the inverted pendulum problem*, Lecture Notes in Computational Science and Engineering, vol. **44**, Springer, (2005), 241–261.
[34] M. E. Tuckermann, B. J. Berne and G. J. Martyna, *Reversible multiple time scale molecular dynamics*, J. Chem. Phys., **97** (1992), 1990–2001.

Received December 2008; revised May 2009.

E-mail address: lebris@cermics.enpc.fr
E-mail address: legoll@lami.enpc.fr